

Chiral-Imbalance Density Wave in Baryonic Matters

Mamiya Kawaguchi*¹ and Shinya Matsuzaki†²

¹ *Department of Physics, Nagoya University, Nagoya 464-8602, Japan.*

² *Center for Theoretical Physics and College of Physics, Jilin University, Changchun, 130012, China*
(Dated: March 26, 2019)

We propose a new chirality-imbalance phenomenon arising in baryonic/high dense matters under a magnetic field. A locally chiral-imbalanced (parity-odd) domain can be created due to the electromagnetically induced $U(1)_A$ anomaly in high-dense matters. The proposed local-chiral imbalance generically possesses a close relationship to a spacial distribution of an inhomogeneous chiral (pion)-vector current coupled to the magnetic field. To demonstrate such a nontrivial correlation, we take the skyrmion crystal approach to model baryonic/high dense matters. Remarkably enough, we find the chirality-imbalance distribution takes a wave form in a high density region (dubbed “*chiral-imbalance density wave*”), when the inhomogeneous chiral condensate develops to form a chiral density wave. This implies the emergence of a nontrivial density wave for the explicitly broken $U(1)_A$ current simultaneously with the chiral density wave for the spontaneously broken chiral-flavor current. We further find that the topological phase transition in the skyrmion crystal model (between skyrmion and half-skyrmion phases) undergoes the deformation of the chiral-imbalance density wave in shape and periodicity. The emergence of this chiral-imbalance density wave could give a crucial contribution to studies on the chiral phase transition, as well as the nuclear matter structure, in compact stars under a magnetic field.

I. INTRODUCTION

Exploring the properties of QCD under an extreme environment has attracted a lot of attentions to extract a novel insight of the nonperturbative nature of QCD involving the chiral-symmetry breaking structure. Particularly, it would be important to ask how much the $U(1)_A$ breaking (anomaly) can serve as a source for the baryonic matter structure, while competing with contributions from the spontaneous breaking of the chiral symmetry, which would also be linked to the origin of the nucleon mass.

Regarding a nontrivial issue on the $U(1)_A$ anomaly under exotic environments, it has been expected [1–16] in the hot QCD system that the local-parity-odd domain would show up due to the nonzero chirality (sometimes called the chiral-charge separation) induced by the anomalous $U(1)_A$ current coupled to the topological gluon configuration (sphaleron [17, 18]). This local P -odd domain, called the chiral-imbalance medium [19], is expected to be observed as the nontrivial consequences for the presence of the $U(1)_A$ anomaly (and/or strong CP violation) in heavy ion collisions, although being metastable to be gone after the typical time scale of QCD lasts [19–23]. Such a chiral imbalance medium is characterized by the chiral (axial) chemical potential (often denoted by μ_5), and has so far extensively been searched based on various arguments in hot QCD matter applied to heavy ion collision experiments, e.g. [1–16] and [24–31].

In place of invoking the gluonic $U(1)_A$ anomaly, a lo-

cal chiral-imbalance medium can actually be created even in other specific environments apart from QCD. For instance, weak interactions generically break the parity and lead to the chirality imbalance. Indeed, it has recently been shown [32–37] that the chirality imbalance for weakly interacting leptons can be generated in a process of supernova explosions, through the chiral transport mechanism acting on neutrinos. Moreover, a signal induced from the chiral imbalance medium (so-called the chiral magnetic effect) has actually been observed in a condense matter system, called Weyl semimetals [38–40]. Thus, understanding of the chirality imbalance as well as the $U(1)_A$ anomaly has recently been developing and is currently getting interdisciplinary.

In this paper, we propose a novel possibility to create a (stable) chiral-imbalance medium in a high dense QCD with a strong magnetic field. Our central idea is built on a simple observation as follows.

In zero-temperature environment, the topologically nontrivial gluon configuration will not survive longer enough to stay in the QCD time scale, due to the gigantic exponential suppression form of the instanton configuration. Thereby, the $U(1)_A$ anomaly of the gluon-field strength form $\sim \epsilon_{\mu\nu\rho\sigma} G^{\mu\nu} G^{\rho\sigma}$ is supposed to undetectable, in contrast to the finite temperature case with the QCD sphaleron configuration. Instead of the gluonic contribution, the chiral imbalance for quarks can be induced by the electromagnetic $U(1)_A$ anomaly, where the $U(1)_A$ symmetry is explicitly broken by coupling the chiral quarks to the electromagnetic current, yielding the anomaly form like $\epsilon_{\mu\nu\rho\sigma} F^{\mu\nu} F^{\rho\sigma}$, where $F_{\mu\nu}$ stands for the electromagnetic field strength.

Now, consider a high-dense matter system under a magnetic field, inside of which charged pions form the pion-vector current $J_\mu^\pi = i(\partial_\mu \pi^+ \pi^- - \pi^+ \partial_\mu \pi^-)$, coupled to the electromagnetic field, and then might also couple

*mkawaguchi@hken.phys.nagoya-u.ac.jp

†synya@jlu.edu.cn

to the electromagnetic $U(1)_A$ anomaly as above. Of importance here is to note that as discussed in [41–44], in a high-dense medium with a strong magnetic field, the pions can locally form condensates, (so-called inhomogeneous chiral condensates), so that the pion-vector current J_μ^π can also have a locally nontrivial distribution in the medium. Suppose the medium to be so high-dense like that, in such a way that the dense matter can be highly compressed to be almost static. In that case, we may expect to have a local-chiral density ($\rho_5(\vec{x})$ with \vec{x} being three-dimensional spatial vector) associated with the $U(1)_A$ anomaly in the high-dense medium, like

$$\begin{aligned} \rho_5(\vec{x}) &\sim \epsilon^{0\mu\nu\rho} J_\mu^\pi(\vec{x}) F_{\nu\rho}(\vec{x}) / f_\pi^2 \\ &\sim \vec{J}^\pi(\vec{x}) \cdot \vec{B}(\vec{x}) / f_\pi^2. \end{aligned} \quad (\text{I.1})$$

The nonzero ρ_5 in Eq.(I.1) manifestly implies the emergence of a chirality-imbalance driven in the presence of a magnetic field and a nontrivial spatial distribution for a pion-vector current. In fact, one could immediately find the existence of the interaction terms as in Eq.(I.1), once writing down the conventional chiral Lagrangian including the chiral anomaly part: the interaction terms of this type can be generated via the Wess-Zumino-Witten (WZW) term [45, 46], when the $U(1)_A$ charge and the isospin charge plus baryon number are gauged to be identified with the chiral chemical potential μ_5 and the electromagnetic charge for quarks, respectively. Then the functional derivative of the chiral Lagrangian with respect to the μ_5 will immediately lead to the chiral-imbalance density in Eq.(I.1) ^{#1}. Therefore, might it sound trivial? — the answer is “No.”. From Eq.(I.1) one would expect a nontrivial correlation between the presence of the chirality imbalance and the inhomogeneity of the pion-vector current (arising from the inhomogeneous chiral condensate) in medium. That is, Eq.(I.1) would provide a significant possibility to examine *how much the $U(1)_A$ anomaly can be correlated with the spontaneously broken chiral symmetry, by setting the chiral dynamics in a high-dense medium with use of a magnetic field as the probe.*

To monitor a nontrivial physics derived from the ρ_5 in Eq.(I.1), in this paper we take the skyrmion crystal approach [49, 50] as a candidate effective model for describing the baryonic/high-dense matter. In the skyrmion crystal approach, the baryonic matter is described by putting the skyrmions on lattice vertices of a crystal structure. Actually, the large- N_c QCD supports that a topologically-static soliton arising as a skyrmion can be regarded as a baryon [46, 51]. By using the skyrmion

crystal approach, the baryonic matter can also be described as the topologically static-object. In high density region, where baryons is so compressed to be a static object, the skyrmion crystal is a powerful approach for the qualitative-baryon description ^{#2} as if they could form crystals [44, 53–61].

The skyrmion crystal picture is indeed in accord with the desired setup for the emergence of a local-chirality imbalance proposed in Eq.(I.1). Besides, the skyrmion crystal approach predicts a characteristic phenomena which is called “topological phase transition” (for reviews see e.g., Refs. [57–59]). If we choose the underlying structure as the face-centered-cubic (FCC) crystal, the crystal configuration is changed from a FCC crystal to a cubic-centered crystal (CC). Actually, it has been indicated that the results from effective field theories, in which such a topological phase transition is encoded, can be consistent with the present observation of neutron star physics [62–64]. Those facts would give us another interesting chance to investigate some correlations between the chirality imbalance and the baryonic matter structure.

We demonstrate that a nontrivial correlation between the chiral imbalance distribution and the baryonic/high-dense matter structure actually shows up: it turns out that the ρ_5 as in Eq.(I.1) emerges to form a density wave, simultaneously with a chiral density wave for a pion-vector current J_μ^π . It is dubbed “*chiral-imbalance density wave*”. We also observe that the periodicity of the chiral-imbalance density wave harmonizes to almost coincide with the previously proposed inhomogeneous-chiral condensate distributions induced on the skyrmion crystal [44].

The emergence of this chiral-imbalance density wave would significantly contribute to studies on the chiral phase transition under a magnetic field with the inhomogeneous chiral condensates (chiral density waves) incorporated, as has been discussed in [41–43] in different setup for chiral effective models, and also on the nuclear matter structure, in compact stars holding a magnetic field.

This paper is organized as follows: In Sec. II we start with introduction of our target model-setup, by reviewing the skyrmion crystal approach for modeling of baryonic matters. This part also includes introduction of a magnetic field and a chiral chemical potential in the chiral effective model, so as to examine the chirality imbalance induced by a magnetic field. Then we explicitly see that the chiral imbalance density as proposed in Eq.(I.1) indeed shows up in the present setup. Quantities related to the inhomogeneous chiral condensate as well as the baryon number density are also derived there. Sec. III provides

^{#1} Several discussions on chirality-imbalance effects, induced with a strong magnetic field for hadron physics, arising through the WZW term, have been made so far [47, 48]. However, to our best knowledge, no references have picked up the interaction term as in Eq.(I.1), which involves the pion-vector current part, instead of the external photon field.

^{#2} Going beyond such qualitative arguments on the baryon description, it has recently been suggested that the skyrmion approach could quantitatively be consistent with realistic light nuclei with a desirable size of the binding energy [52].

the numerical analysis on the chiral imbalance distributions in the skyrmion crystal, and shows the emergence of the chiral-imbalance density wave, and several related phenomena, such as correlation with the inhomogeneity of the chiral condensate. Conclusion for the present paper is given in Sec.IV. Appendix A compensates knowledge on symmetry properties for the chiral-imbalance distribution and the inhomogeneous chiral condensate, in the skyrmion crystal.

II. CHIRALITY IMBALANCE IN SKYRMION CRYSTAL UNDER A MAGNETIC FIELD

In this section, we first introduce preliminary setups in studying the magnetic properties of the skyrmion crystal, such as the basic construction in the chiral limit (Part A) and see how the baryon number density is modified by the presence of a magnetic field which explicitly breaks the chiral symmetry (Part B). And then, we discuss how the magnetic-field driven $U(1)_A$ anomaly induces the chirality imbalance (Part C).

A. Skyrmion crystal approach

The Skyrme model [49] based on the 2-flavor chiral symmetry is described in the chiral limit by the following Lagrangian:

$$\mathcal{L}_{\text{Skyr}} = \frac{f_\pi^2}{4} \text{tr} [\partial_\mu U \partial^\mu U^\dagger] + \frac{1}{32g^2} \text{tr} [U^\dagger \partial_\mu U, U^\dagger \partial_\nu U]^2, \quad (\text{II.2})$$

where U is the chiral field parameterized by the pion fields, f_π the pion decay constant, and g the dimensionless coupling constant. In the skyrmion crystal approach, the chiral field U is parameterized as

$$U = \phi_0 + i\tau_a \phi_a, \quad (\text{II.3})$$

with $a = 1, 2, 3$, τ^a being the Pauli matrices, and the unitary constraint $(\phi_0)^2 + (\phi_a)^2 = 1$. For later convenience, we also introduce unnormalized fields $\bar{\phi}_\alpha$ ($\alpha = 0, 1, 2, 3$), which are related to the corresponding normalized ones through

$$\phi_\alpha = \frac{\bar{\phi}_\alpha}{\sqrt{\sum_{\beta=0}^3 \bar{\phi}_\beta \bar{\phi}_\beta}}. \quad (\text{II.4})$$

We will consider the static skyrmion crystal formed by the static pion fields, $\phi_\alpha(t, x, y, z) = \phi_\alpha(x, y, z)$. In a crystal lattice with a periodicity of $2L$ (the size of the unit cell for a single crystal), the static pion fields can be expanded in terms of the Fourier series [53]:

$$\bar{\phi}_0(x, y, z) = \sum_{a,b,c} \bar{\beta}_{abc} \cos(a\pi x/L) \cos(b\pi y/L) \cos(c\pi z/L)$$

$$\begin{aligned} \bar{\phi}_1(x, y, z) &= \sum_{h,k,l} \bar{\alpha}_{hkl}^{(1)} \sin(h\pi x/L) \cos(k\pi y/L) \cos(l\pi z/L) \\ \bar{\phi}_2(x, y, z) &= \sum_{h,k,l} \bar{\alpha}_{hkl}^{(2)} \cos(l\pi x/L) \sin(h\pi y/L) \cos(k\pi z/L) \\ \bar{\phi}_3(x, y, z) &= \sum_{h,k,l} \bar{\alpha}_{hkl}^{(3)} \cos(k\pi x/L) \cos(l\pi y/L) \sin(h\pi z/L), \end{aligned} \quad (\text{II.5})$$

where h, k and l are taken to be integers. In the present study, we shall construct the FCC crystal from the skyrmion approach. Then we need to impose some constraint conditions on the Fourier coefficient $\bar{\alpha}$ and $\bar{\beta}$ (for more on this, see [53]).

It is also interesting to note that in the skyrmion crystal approach the configuration of the $\phi_\alpha(x, y, z)$ can be rephrased as the inhomogeneous quark condensates like,

$$\begin{aligned} \phi_0(x, y, z) &\sim \langle 0 | \bar{q} q | 0 \rangle (x, y, z) \\ \phi_a(x, y, z) &\sim \langle 0 | \bar{q} i \gamma_5 \tau_a q | 0 \rangle (x, y, z). \end{aligned} \quad (\text{II.6})$$

The skyrmion crystal approach has the characteristic phenomena which is so-called topological phase transition. At some critical lattice size, this phase transition occurs in the skyrmion crystal. As a result, the FCC crystal structure changes to be the CC form. In terms of the phase transition, the low density region with the skyrmion crystal realized as the FCC form is called "skyrmion phase", while the high density region where the CC structure is manifest, called "half-skyrmion phase" [44, 53–61].

B. Baryon number density in a magnetic field

To consider the magnetic effect on the skyrmion crystal, we introduce the external vector field \mathcal{V}_μ and the external axial field \mathcal{A}_μ , by gauging the chiral symmetry,

$$D_\mu U = \partial_\mu U - i[\mathcal{V}_\mu, U] + i\{\mathcal{A}_\mu, U\}. \quad (\text{II.7})$$

The magnetic field (B), the baryon chemical potential (μ_B) and the chiral chemical potential (μ_5) are embedded into the \mathcal{V}_μ and \mathcal{A}_μ ,

$$\begin{aligned} \mathcal{V}_\mu &= Q_B \mu_B \delta_{\mu 0} + e Q_{\text{em}} \mathcal{A}_\mu \\ \mathcal{A}_\mu &= \mu_5 \delta_{\mu 0} \mathbf{1}_{2 \times 2}, \end{aligned} \quad (\text{II.8})$$

where $Q_B = \frac{1}{3} \mathbf{1}_{2 \times 2}$ is the baryon number charge matrix, $Q_{\text{em}} = \frac{1}{6} \mathbf{1}_{2 \times 2} + \frac{1}{2} \tau_3$ the electric charge matrix, and the magnetic field B is incorporated into \mathcal{A}_μ . In this study, we consider a constant magnetic field (B) along the z axis. Then, the magnetic field breaks the $O(3)$ symmetry down to the $O(2)$ symmetry. To respect the residual $O(2)$ symmetry, we choose the following symmetric gauge,

$$\mathcal{A}_\mu = -\frac{1}{2} B y \delta_\mu^1 + \frac{1}{2} B x \delta_\mu^2. \quad (\text{II.9})$$

The covariantized Wess-Zumino-Witten (WZW) action ($\Gamma_{\text{WZW}} = \int d^4x \mathcal{L}_{\text{WZW}}$), which corresponds to the

solution for the non-Abelian $U(2)_L \times U(2)_R$ anomaly equation, makes the baryon number density ρ_B coupled to the baryon chemical potential μ_B . Hence, the ρ_B is given by [65–67]

$$\rho_B = \left. \frac{\partial \mathcal{L}_{\text{wzw}}}{\partial \mu_B} \right|_{\mu_B=0} = \rho_W + \tilde{\rho}_{eB} \quad (\text{II.10})$$

with

$$\begin{aligned} \rho_W &= \frac{1}{24\pi^2} \epsilon^{0\nu\rho\sigma} \text{tr} [(\partial_\nu U \cdot U^\dagger)(\partial_\rho U \cdot U^\dagger)(\partial_\sigma U \cdot U^\dagger)] \\ \tilde{\rho}_{eB} &= \frac{ie}{16\pi^2} \epsilon^{0\nu\rho\sigma} \partial_\sigma (\text{tr}[A_\nu Q_{\text{em}}\{\partial_\rho U, U^\dagger\}]), \end{aligned} \quad (\text{II.11})$$

where ρ_W denotes the winding-number density and $\tilde{\rho}_{eB}$ is the induced baryon number density. By taking the symmetric gauge in Eq.(II.9), ρ_B is evaluated as a function of a set of the topological ϕ_α fields (Eq.(II.3)) as follows:

$$\begin{aligned} \rho_B &= \left. \frac{1}{24\pi^2} \epsilon^{0\nu\rho\sigma} \text{tr} [(\partial_\nu U \cdot U^\dagger)(\partial_\rho U \cdot U^\dagger)(\partial_\sigma U \cdot U^\dagger)] \right|_{\phi_\alpha} \\ &\quad - \frac{eB}{4\pi^2} [(\partial_z \phi_3)\phi_0 - (\partial_z \phi_0)\phi_3] \\ &\quad + \frac{eB}{8\pi^2} (\{[y\partial_y \phi_3]_{\text{disc}}(\partial_z \phi_0) - [y\partial_y \phi_0]_{\text{disc}}(\partial_z \phi_3)\} \\ &\quad - \{(\partial_z \phi_3)[x\partial_x \phi_0]_{\text{disc}} - (\partial_z \phi_0)[x\partial_x \phi_3]_{\text{disc}}\}). \end{aligned} \quad (\text{II.12})$$

Here we have used discretized form with a derivative operator such as $[y\partial_y \phi_3]_{\text{disc}}$ to hold the translational invariance in the skyrmion crystal (the explicit expressions and more details are supplied in [44]).

In the skyrmion crystal approach, the skyrmion crystal configuration can be visualized through the baryon-number density distribution $\rho_B(x, y, z)$. Therefore the external magnetic field deforms the skyrmion configuration due to the existence of the induced baryon number density, as discussed in [44].

C. Induced chiral-imbalance density

Now we discuss how the chirality imbalance shows up under a magnetic field through the $U(1)_A$ anomaly. We first note that in a way similar to the baryon number density, the covariantized WZW action regarding the $U(2)_L \times U(2)_R$ anomaly makes it possible to couple the chirality imbalance functional ρ_5 (hereafter called chiral imbalance distribution) with the chiral chemical potential μ_5 . It arises from the $\mathcal{V} - \mathcal{V} - \mathcal{A}$ type interaction terms, to be

$$\begin{aligned} \rho_5 &= \left. \frac{\partial \mathcal{L}_{\text{wzw}}}{\partial \mu_5} \right|_{\mu_5=0} = \frac{ie}{16\pi^2} \epsilon^{0\nu\rho\sigma} \partial_\nu (\text{tr}[A_\rho Q_{\text{em}}\{\partial_\sigma U, U^\dagger\}]) \\ &= \frac{e}{8\pi^2} \text{tr} \left[Q_{\text{em}} \left\{ \tilde{F}^{0\mu} H_\mu(U) + \tilde{F}^{0\mu}(U) A_\mu \right\} \right], \end{aligned} \quad (\text{II.13})$$

where $H_\mu(U) = i[\partial_\mu U, U^\dagger]$ denotes a pion-vector current field (sometimes called a chiral connection field) and $\tilde{F}^{0\mu} \equiv \frac{1}{2}\epsilon^{0\mu\nu\rho} F_{\nu\rho}$ is a generic magnetic field strength. Thus the chiral imbalance density ρ_5 is supplied by the pionic vector current coupled to the external magnetic field.

At this moment, we have arrived at our central formula, Eq.(II.13), which is a generalization form for Eq.(I.1). Indeed, this is in accord with the form of the $U(1)_A$ anomaly $\sim \tilde{F}_{\mu\nu} F^{\mu\nu}$, where one of the field strength $F_{\mu\nu}$ is replaced by the one constructed from the pionic-vector current $H_\mu(U)$.

Projecting the generic formula of Eq.(II.13) onto the skyrmion crystal approach, we see that the ρ_5 is expressed by a set of skyrmion configurations parametrized by the topological ϕ_α fields, as in Eq.(II.3). Under the symmetric gauge in Eq.(II.9), the chiral imbalance distribution ρ_5 is thus evaluated as

$$\begin{aligned} \rho_5 &= \frac{eB}{4\pi^2} \{(\partial_z \phi_1)\phi_2 - (\partial_z \phi_2)\phi_1\} \\ &\quad + \frac{eB}{8\pi^2} ([x\partial_x \phi_1]_{\text{disc}} + [y\partial_y \phi_1]_{\text{disc}})(\partial_z \phi_2) \\ &\quad - \frac{eB}{8\pi^2} ([x\partial_x \phi_2]_{\text{disc}} + [y\partial_y \phi_2]_{\text{disc}})(\partial_z \phi_1). \end{aligned} \quad (\text{II.14})$$

Here we have used the discretized form in similar way to Eq.(II.12). Crucial to note here is that no chirality imbalance distribution emerges without nonzero magnetic field. Note also that the space averaged value of ρ_5 goes to zero: $\int_{\text{cube}} d^3x \rho_5 = 0$. This is because of the parity-odd property. (Or, more generically, it is due to the fact that no nontrivial configuration is presented for the external gauge field A_μ at the boundary of the target cube. See Eq.(II.13).) Hence, these facts imply that the skyrmion crystal is turned into the local-chiral imbalance medium by the presence of a magnetic field, in which the local-chiral imbalance distribution would be expected to have a nontrivial correlation with the local-inhomogeneous chiral condensates in Eq.(II.6), as well as the local-baryon number density distribution given by ρ_B in Eq.(II.12).

III. NUMERICAL RESULTS

In this section we numerically examine the chiral imbalance distribution ρ_5 in Eq.(II.14) and make an attempt to find its nontrivial correlation with the baryon matter structure, based on the skyrmion crystal approach under a magnetic field. The baryon matter structure can be monitored by examining the position dependence of ρ_B in Eq. (II.12), and the chiral imbalance distribution ρ_5 by Eq.(II.14). We then note that the baryon number density ρ_B and the chiral imbalance distribution ρ_5 are expressed as the function of the Fourier coefficients $\tilde{\beta}_{abc}$ and $\tilde{\alpha}_{hkl}^{(i)}$, as seen from Eq. (II.5). There the Fourier coefficients are determined by minimizing the per-baryon energy $E/N_B = -\frac{1}{4} \int_{\text{cube}} d^3x \mathcal{L}_{\text{Skyr}}$, with N_B having been

taken to be 4, and $\int_{\text{cube}} = \int_{-L}^L dx \int_{-L}^L dy \int_{-L}^L dz$. (Note that the magnetically induced $\tilde{\rho}_{eB}$ in Eq.(II.11) vanishes in the integral, because of the trivial configuration for the gauge field A_μ at the boundary of the target cube, hence it does not affect the total baryon number at all.) Then, the per-baryon energy is also expressed as a function of the Fourier coefficients $\tilde{\beta}_{abc}, \tilde{\alpha}_{hkl}^{(i)}$ which are used as variational parameters in the numerical calculation. Once the strength of a magnetic field is fixed, the Fourier coefficients for a given set of crystal size L is determined by minimizing the per-baryon energy. Thus, the Fourier coefficients $\tilde{\beta}_{abc}, \tilde{\alpha}_{hkl}^{(i)}$ depend on the crystal size L and a magnetic field scale eB . For numerical computations, we take $f_\pi = 92.4$ MeV and $g = 5.93$ as inputs [58].

A. Chiral imbalance distribution on the skyrmion crystal: chiral-imbalance density wave

In this subsection we examine the chirality imbalance on the skyrmion crystal configuration in the presence of a magnetic field, which can be visualized through the chiral imbalance distribution, ρ_5 , and the baryon-number density distribution, ρ_B , respectively.

In Figs. 1 and 2, we plot the skyrmion crystal configurations and the chiral imbalance distribution ρ_5 in a low density region where $L = 2.0$ fm (corresponding to the skyrmion phase), with the magnetic field scale fixed to 400 MeV and 800 MeV, respectively. The magnitude of ρ_5 has been amplified by multiplying a factor of 10, because of its smallness compared to the baryon number density ρ_B .

First, see the left panels in the figures (the panels (a)), showing the skyrmion crystal configurations characterized by the baryon number density ρ_B under a magnetic field. We then find that even in the presence of a magnetic field, the skyrmion crystal keeps the FCC structure, as was discussed in [44].

Looking at the middle panels (b) in Figs. 1 and 2: one realizes that remarkably nontrivial phenomenon has been emergent. These panels display the chiral imbalance distributions in the skyrmion crystal, and show that the chirality imbalance shows up on the skyrmion crystal to be locally distributed on the FCC crystal configuration. Interesting enough, such a chiral imbalance distribution looks like forming a wave (with odd parity). This can be dubbed “*chiral-imbalance density wave*”, which flows quite differently from the baryon number density on the crystal.

From the left panels in the figures (panels (c)), we also see that the magnitude of the chiral imbalance distribution gets bigger, as a magnetic field increases, which is simply expected from the form of the functional of ρ_5 in Eq.(II.14).

Next, in Figs. 3 and 4, we draw the skyrmion configurations and the chiral imbalance distribution in a high density region where $L = 1.0$ fm (corresponding to the half-skyrmion phase), with $\sqrt{eB} = 400$ and 800 MeV, respectively. At the first glance, one immediately finds that as a magnetic field gets bigger, the CC configuration dramatically becomes distorted (Figs. 3(a) and 4(a)), as was observed in [44].

As for the chiral imbalance distribution, again, the configuration of ρ_5 forms a wave (the chiral-imbalance density wave), which, however, looks quite similar to the skyrmion configuration except for the parity property. This is in contrast to the case of the skyrmion phase, as depicted in Figs. 3(b) and 4(b). This observation indicates a nontrivial consequence that the topological phase transition leads to the change of the chiral-imbalance density wave in shape.

Similarly to the case for the skyrmion phase, Figs. 3(c) and 4(c) also show that the chiral imbalance distribution grows up as the baryonic matter approaches a higher-intense object influenced by a strong magnetic field (with $\sqrt{eB} = 800$ MeV).

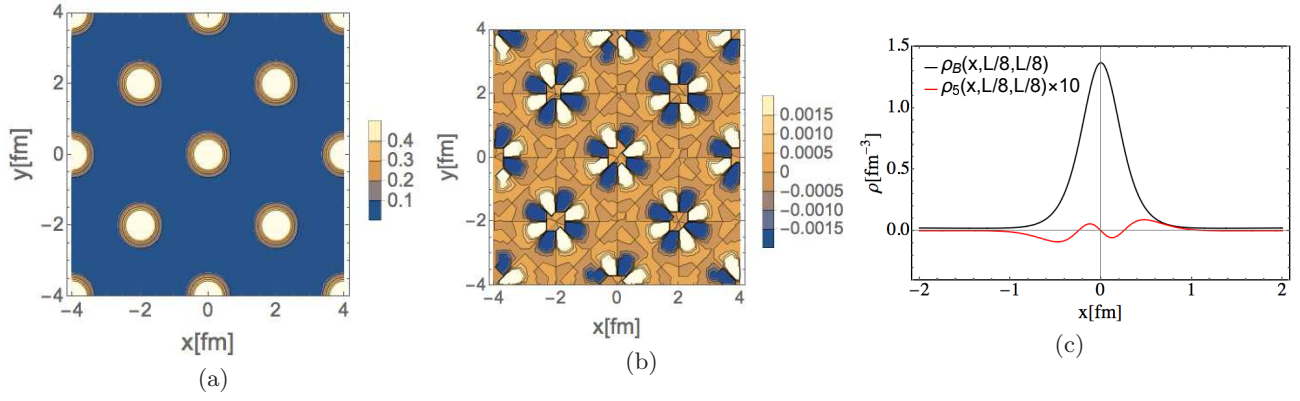


FIG. 1: The chiral imbalance distribution on the skyrmion configuration at $L = 2.0$ [fm] for $\sqrt{eB} = 400$ [MeV]. (a) The contour plot of the skyrmion configuration on the x - y plane, $\rho_B(x, y, L/8)$. (b) The contour plot of the chiral imbalance distribution on the x - y plane, $\rho_5(x, y, L/8)$. (c) The distribution of the skyrmion and the chiral imbalance along the x axis specified at $y = z = L/8 = 0.25$ [fm].

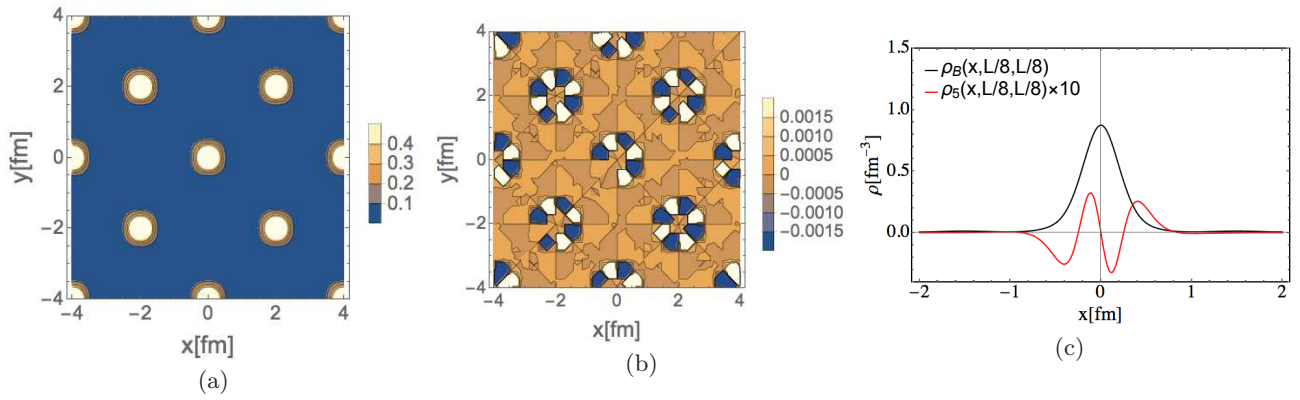


FIG. 2: The chiral imbalance distribution on the skyrmion configuration at $L = 2.0$ [fm] for $\sqrt{eB} = 800$ [MeV]. (a) The contour plot of the skyrmion configuration on the x - y plane, $\rho_B(x, y, L/8)$. (b) The contour plot of the chiral imbalance distribution on the x - y plane, $\rho_5(x, y, L/8)$. (c) The distribution of the skyrmion and the chiral imbalance along the x axis specified at $y = z = L/8 = 0.25$ [fm].

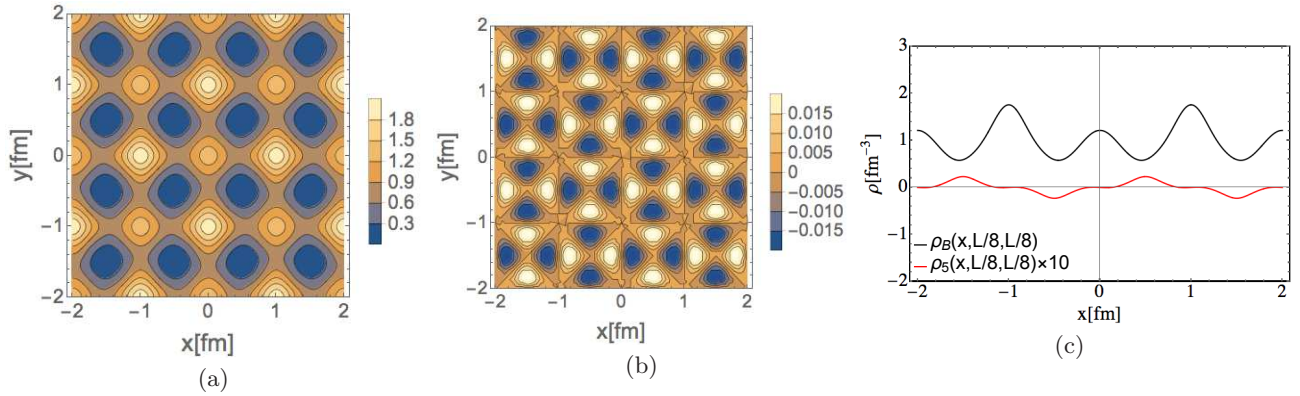


FIG. 3: The chiral imbalance distribution on the skyrmion configuration at $L = 1.0$ [fm] for $\sqrt{eB} = 400$ [MeV]. (a) The contour plot of the skyrmion configuration on the x - y plane, $\rho_B(x, y, L/8)$. (b) The contour plot of the chiral imbalance distribution on the x - y plane, $\rho_5(x, y, L/8)$. (c) The distribution of the skyrmion and the chiral imbalance along the x axis specified at $y = z = L/8 = 0.125$ [fm].

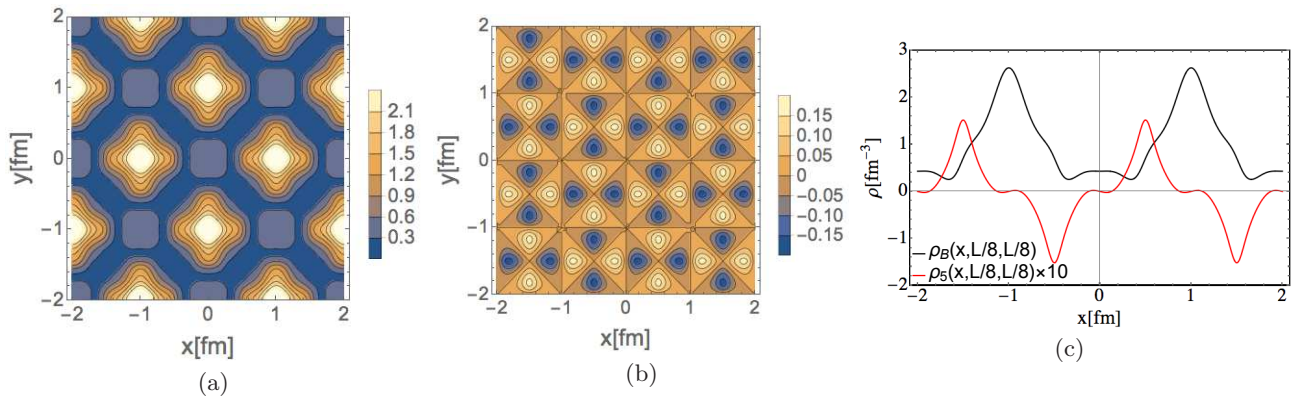


FIG. 4: The chiral imbalance distribution on the skyrmion configuration at $L = 1.0[\text{fm}]$ for $\sqrt{eB} = 800[\text{MeV}]$. (a) The contour plot of the skyrmion configuration on the x - y plane, $\rho_B(x, y, L/8)$. (b) The contour plot of the chiral imbalance distribution on the x - y plane, $\rho_5(x, y, L/8)$. (c) The distribution of the skyrmion and the chiral imbalance along the x axis specified at $y = z = L/8 = 0.125[\text{fm}]$.

B. Chiral-imbalance density wave and chiral density wave

In the previous work done by authors [44], a possible correlation between the inhomogeneous quark condensate and the deformation of the skyrmion crystal form was addressed. In this subsection, we shall further show a remarkable presence of a nontrivial correlation between the chiral imbalance distribution, i.e., the chiral-imbalance density wave, and the inhomogeneous-chiral condensate distribution, i.e., a chiral density wave, as was observed in [44]. As to the latter distribution, we may select the inhomogeneity of ϕ_1 associated with the inhomogeneous quark condensate (see Eq.(II.6)). This is because among the inhomogeneous chiral condensates $\sim \phi^\alpha$ in Eq.(II.6), only the ϕ_1 has the same parity property as the ρ_5 along the x -direction (see Eq.(II.5)), hence it is most convenient to compare the ρ_5 distribution with that of the ϕ_1 along the x -axis as has been depicted in the distribution plots so far.

Before proceeding the comparison between the ρ_5 and the ϕ_1 , we first note from Figs 1, 2, 3, and 4 that the magnitude of the chiral-inhomogeneous density wave is much smaller (by a factor of 10) than the baryon number distribution (skyrmion configuration) in the system. Though it implies a small $U(1)_A$ anomaly effect, we may try to see how the local chirality imbalance is responsible for the nonzero inhomogeneity of ϕ_1 , in both the skyrmion and half-skyrmion phases, by comparing the wave forms and the peak structures for the chiral-inhomogeneous density wave and a chiral density wave. The observation like this would deduce a quantitative understanding on how much the $U(1)_A$ anomaly effect is encoded in the chiral condensate. To easily see and visually grasp a nontrivial correlation in such peak structures by eyes, we may amplify the amplitude of ρ_5 in the (half-) skyrmion phase,

by a factor defined as

$$C_{400(800)}^{(h-)\text{skyr}} \equiv \frac{\phi_1^{\max}(\bar{x}, y = z = L/8)|_{\sqrt{eB}=400(800)\text{ MeV}}}{\rho_5^{\max}(\bar{x}, y = z = L/8)|_{\sqrt{eB}=400(800)\text{ MeV}}}, \quad (\text{III.15})$$

where “max” denotes the maximum value realized at $(x, y, z) = (\bar{x}, L/8, L/8)$ for given \sqrt{eB} (in which the \bar{x} is just a number, to be read off). Thus, the amplified chiral-imbalance distribution, $(\rho_5 \times C_{400(800)}^{(h-)\text{skyr}})$, is set to a dimensionless quantity as well as the ϕ_1 , and can have the same order of magnitude as what the ϕ_1 can have.

In Fig. 5 we plot the amplified chiral-imbalance distributions, $(\rho_5 \times C_{400(800)}^{\text{skyr}})$, and the inhomogeneity distributions for ϕ_1 , in the skyrmion and half-skyrmion phases, respectively. From this figure, we find the following features:

- As the strength of a magnetic field increases, the inhomogeneity of ϕ_1 tend to be localized and the amplitude of ϕ_1 becomes small, as discussed in [44].
- As for the correlation between the chiral-imbalance density wave and a chiral density wave depicted by the inhomogeneity of ϕ_1 , the peak point for the former does not match with that of the ϕ_1 -chiral density wave.

Moving on to the half-skyrmion phase, we make plots of the amplified chiral-imbalance distribution, $\rho_5 \times C_{400(800)}^{h\text{-skyr}}$, and the inhomogeneities of ϕ_1 in Fig. 6. The figure tells us the following characteristic properties:

- In contrast to the skyrmion phase, the magnetic effect is insensitive to the inhomogeneous configuration of ϕ_1 , as discussed in [44].
- The periodicity of the chiral-imbalance density wave $(\rho_5 \times C_{400(800)}^{h\text{-skyr}})$ synchronizes with a chiral den-

sity wave formed by the ϕ_1 inhomogeneity for any strength of a magnetic field.

It is of particular interest to note from the second item that in the half-skyrmion phase the presence of a magnetic field makes a nontrivial correlation between the chirality imbalance and the inhomogeneous quark condensate, in terms of the periodicity for density wave distributions. Actually, the coincidence of the periodicity in the half-skyrmion phase can analytically be understood as by the symmetry properties for the ρ_5 and ϕ_1 on crystals given

in Eqs. (A.1) - (A.4), in Appendix A.

Those nontrivial-wave correlations having a different aspect between the skyrmion and half-skyrmion phases would provide us with a novel possibility: the presence of the chiral-imbalance density wave as a consequence of the $U(1)_A$ anomaly would be an important probe for the phase boundary between the skyrmion and half-skyrmion phases in the high-dense baryonic matter under a magnetic field.

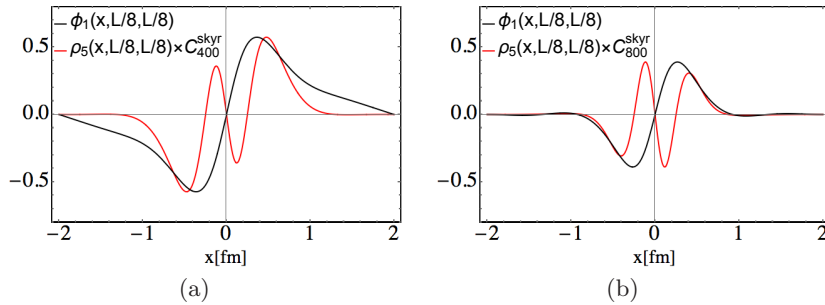


FIG. 5: The distribution of $\phi_1(x, L/8, L/8)$ and $\rho_5(x, L/8, L/8) \times C_{400(800)}^{\text{skyr}}$ in the skyrmion phase where $L = 2.0[\text{fm}]$ for $\sqrt{eB} = 400[\text{MeV}]$ (a) and $\sqrt{eB} = 800[\text{MeV}]$ (b).

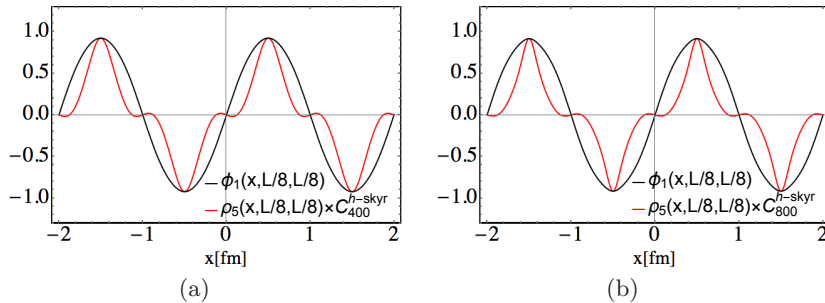


FIG. 6: The distribution of $\phi_1(x, L/8, L/8)$ and $\rho_5(x, L/8, L/8) \times C_{400(800)}^{(h-)\text{skyr}}$ in the half-skyrmion phase where $L = 1.0[\text{fm}]$ for $\sqrt{eB} = 400[\text{MeV}]$ (a) and $\sqrt{eB} = 800[\text{MeV}]$ (b).

IV. CONCLUSIONS

In summary, we proposed a novel possibility to create a chiral-imbalance medium in a high dense baryonic matter under a magnetic field. It is a chirality-imbalance that can be emerged due to the magnetic $U(1)_A$ anomaly coupled with a local-nontrivial inhomogeneity of a pion-vector current arising in the high-dense matter system, as was roughly sketched in the introductory part of the present paper (Eq.(I.1)). This imbalance is in contrast to the conventional one generated by the gluonic $U(1)_A$ anomaly in the case of hot QCD matter. Hence it would

provide a new chance to examine how much the $U(1)_A$ anomaly can be relevant to the net chiral asymmetry, compared to the spontaneously broken chiral symmetry.

To demonstrate the crucial contribution of the proposed chiral-imbalance in Eq.(I.1), in the present paper we have taken the skyrmion crystal approach to make a model description for baryonic/high dense matters, to explicitly show that a nontrivial chiral imbalance distribution can indeed be induced in the modeled skyrmion crystal, due to the presence of a magnetic field. Interestingly enough, the chiral imbalance distribution turned out to take a wave form in a high density region, when

the inhomogeneous chiral condensate develops to form a chiral density wave. This implies the emergence of a non-trivial density wave for the explicitly broken $U(1)_A$ current simultaneously with the chiral density wave for the spontaneously broken chiral-flavor current. This emergent wave was dubbed “*chiral-imbalance density wave*”.

We further observed that the topological phase transition in the skyrmion crystal model (between the skyrmion and half-skyrmion phases) leads to the change of the chiral-imbalance density wave in shape. In particular, it was shown that in the half-skyrmion phase, the periodicity of the chirality-imbalance distribution synchronizes with the inhomogeneous chiral condensate, in contrast to the case of the skyrmion phase where the chiral-imbalance density wave flows with a different periodicity from a chiral density wave.

The emergence of the chiral-imbalance density wave in dense matters could give a crucial contribution to studies on the chiral phase transition, as well as the nuclear matter structure, in compact stars under a magnetic field, and would give a significant impact on analyses regarding the inhomogeneous chiral condensate through introducing the chiral density wave, as was mentioned in Introduction of the present paper.

Also, our findings would make an important step to make deeper understanding of the role of the $U(1)_A$ anomaly in a sense of the origin of baryon mass as well as the baryon matter structure, and would give some impacts on an interdisciplinary physics like those raised in Introduction of this paper, e.g. the chirality imbalance for chiral neutrinos in supernova explosions and similar related chiral transport physics in dense matter systems.

Acknowledgments

We are grateful to Yong-Liang Ma for several useful comments. This work was supported in part by the JSPS Grant-in-Aid for Young Scientists (B) No. 15K17645 (S.M.), National Science Foundation of China (NSFC) under Grant No. 11747308 (S.M.), and the Seeds Funding of Jilin University (S.M.). K.M. was also partially supported by the JSPS Grant-in-Aid for JSPS Research Fellow No. 18J1532.

Appendix A: Translational symmetries for ρ_5 and ϕ_1

In this Appendix, we provide a supplement on the translational symmetry properties for ρ_5 and ϕ_1 , which can help understand the coincidence for the periodicity among them in the half-skyrmion phase, as has been observed in Fig. 6.

Under the translational symmetry, ρ_5 transforms in the following way: in skyrmion phase with the FCC structure, we have

$$\rho_5(x, y, z) = \rho_5(x + L, y, z)$$

$$= -\rho_5(x + L, y, z + L) = -\rho_5(x, y + L, z + L), \quad (\text{A.1})$$

while in half-skyrmion phase with the CC structure, we have

$$\begin{aligned} \rho_5(x, y, z) &= -\rho_5(x + L, y, z) \\ &= -\rho_5(x, y + L, z) = \rho_5(x, y, z + L). \end{aligned} \quad (\text{A.2})$$

Under the translational symmetry, ϕ_1 transforms as follows: in skyrmion phase with the FCC structure, we have

$$\begin{aligned} \phi_1(x, y, z) &= -\phi_1(x + L, y + L, z) \\ &= -\phi_1(x + L, y, z + L) = \phi_1(x, y + L, z + L), \end{aligned} \quad (\text{A.3})$$

while in half-skyrmion phase with the CC structure, we have

$$\begin{aligned} \phi_1(x, y, z) &= -\phi_1(x + L, y, z) \\ &= \phi_1(x, y + L, z) = \phi_1(x, y, z + L). \end{aligned} \quad (\text{A.4})$$

-
- [1] D. Kharzeev, A. Krasnitz and R. Venugopalan, Phys. Lett. B **545**, 298 (2002) doi:10.1016/S0370-2693(02)02630-8 [hep-ph/0109253].
- [2] D. Kharzeev and A. Zhitnitsky, Nucl. Phys. A **797**, 67 (2007) doi:10.1016/j.nuclphysa.2007.10.001 [arXiv:0706.1026 [hep-ph]].
- [3] D. E. Kharzeev, L. D. McLerran and H. J. Warringa, Nucl. Phys. A **803**, 227 (2008) doi:10.1016/j.nuclphysa.2008.02.298 [arXiv:0711.0950 [hep-ph]].
- [4] K. Fukushima, D. E. Kharzeev and H. J. Warringa, Phys. Rev. D **78**, 074033 (2008) doi:10.1103/PhysRevD.78.074033 [arXiv:0808.3382 [hep-ph]].
- [5] D. T. Son and P. Surowka, Phys. Rev. Lett. **103**, 191601 (2009) doi:10.1103/PhysRevLett.103.191601 [arXiv:0906.5044 [hep-th]].
- [6] D. E. Kharzeev and H. U. Yee, Phys. Rev. D **83**, 085007 (2011) doi:10.1103/PhysRevD.83.085007 [arXiv:1012.6026 [hep-th]].
- [7] Y. Burnier, D. E. Kharzeev, J. Liao and H. U. Yee, Phys. Rev. Lett. **107**, 052303 (2011) doi:10.1103/PhysRevLett.107.052303 [arXiv:1103.1307 [hep-ph]].
- [8] M. Hongo, Y. Hirono and T. Hirano, Phys. Lett. B **775**, 266 (2017) doi:10.1016/j.physletb.2017.10.028 [arXiv:1309.2823 [nucl-th]].
- [9] H. U. Yee and Y. Yin, Phys. Rev. C **89**, no. 4, 044909 (2014) doi:10.1103/PhysRevC.89.044909 [arXiv:1311.2574 [nucl-th]].
- [10] Y. Hirono, T. Hirano and D. E. Kharzeev, arXiv:1412.0311 [hep-ph].
- [11] L. Adamczyk *et al.* [STAR Collaboration], Phys. Rev. Lett. **114**, no. 25, 252302 (2015) doi:10.1103/PhysRevLett.114.252302 [arXiv:1504.02175 [nucl-ex]].
- [12] Y. Yin and J. Liao, Phys. Lett. B **756**, 42 (2016) doi:10.1016/j.physletb.2016.02.065 [arXiv:1504.06906 [nucl-th]].
- [13] X. G. Huang, Rept. Prog. Phys. **79**, no. 7, 076302 (2016) doi:10.1088/0034-4885/79/7/076302 [arXiv:1509.04073 [nucl-th]].
- [14] D. E. Kharzeev, J. Liao, S. A. Voloshin and G. Wang, Prog. Part. Nucl. Phys. **88**, 1 (2016) doi:10.1016/j.ppnp.2016.01.001 [arXiv:1511.04050 [hep-ph]].
- [15] K. Hattori and X. G. Huang, Nucl. Sci. Tech. **28**, no. 2, 26 (2017) doi:10.1007/s41365-016-0178-3 [arXiv:1609.00747 [nucl-th]].
- [16] S. Shi, Y. Jiang, E. Lilleskov and J. Liao, Annals Phys. **394**, 50 (2018) doi:10.1016/j.aop.2018.04.026 [arXiv:1711.02496 [nucl-th]].
- [17] N. S. Manton, Phys. Rev. D **28**, 2019 (1983). doi:10.1103/PhysRevD.28.2019
- [18] F. R. Klinkhamer and N. S. Manton, Phys. Rev. D **30**, 2212 (1984). doi:10.1103/PhysRevD.30.2212
- [19] L. D. McLerran, E. Mottola and M. E. Shaposhnikov, Phys. Rev. D **43**, 2027 (1991). doi:10.1103/PhysRevD.43.2027
- [20] G. D. Moore, Phys. Lett. B **412**, 359 (1997) doi:10.1016/S0370-2693(97)01046-0 [hep-ph/9705248].
- [21] G. D. Moore and K. Rummukainen, Phys. Rev. D **61**, 105008 (2000) doi:10.1103/PhysRevD.61.105008 [hep-ph/9906259].
- [22] D. Bodeker, G. D. Moore and K. Rummukainen, Phys. Rev. D **61**, 056003 (2000) doi:10.1103/PhysRevD.61.056003 [hep-ph/9907545].
- [23] R. Derradi de Souza, T. Koide and T. Kodama, Prog. Part. Nucl. Phys. **86**, 35 (2016) doi:10.1016/j.ppnp.2015.09.002 [arXiv:1506.03863 [nucl-th]].
- [24] A. A. Andrianov, V. A. Andrianov, D. Espriu and X. Planells, Phys. Lett. B **710**, 230 (2012) doi:10.1016/j.physletb.2012.02.072 [arXiv:1201.3485 [hep-ph]].
- [25] A. A. Andrianov, D. Espriu and X. Planells, Eur. Phys. J. C **73**, no. 1, 2294 (2013) doi:10.1140/epjc/s10052-013-2294-0 [arXiv:1210.7712 [hep-ph]].
- [26] M. Kawaguchi, M. Harada, S. Matsuzaki and R. Ouyang, Phys. Rev. C **95**, no. 6, 065204 (2017) doi:10.1103/PhysRevC.95.065204 [arXiv:1612.00616 [nucl-th]].
- [27] A. A. Andrianov, V. A. Andrianov, D. Espriu, A. E. Putilova and A. V. Iakubovich, Acta Phys. Polon. Supp. **10**, 977 (2017) doi:10.5506/APhysPolBSupp.10.977 [arXiv:1707.06150 [hep-ph]].
- [28] A. A. Andrianov, V. A. Andrianov, D. Espriu, A. V. Iakubovich and A. E. Putilova, EPJ Web Conf. **158**, 03012 (2017) doi:10.1051/epjconf/201715803012 [arXiv:1710.01760 [hep-ph]].
- [29] A. A. Andrianov, V. A. Andrianov, D. Espriu, A. V. Iakubovich and A. E. Putilova, Phys. Part. Nucl. Lett. **15**, no. 4, 357 (2018). doi:10.1134/S1547477118040027
- [30] A. E. Putilova, A. V. Iakubovich, A. A. Andrianov, V. A. Andrianov and D. Espriu, EPJ Web Conf. **191**, 05014 (2018). doi:10.1051/epjconf/201819105014
- [31] A. A. Andrianov, V. A. Andrianov, D. Espriu, A. V. Iakubovich and A. E. Putilova, arXiv:1902.10705 [hep-ph].
- [32] J. Charbonneau and A. Zhitnitsky, JCAP **1008**, 010 (2010) doi:10.1088/1475-7516/2010/08/010 [arXiv:0903.4450 [astro-ph.HE]].
- [33] D. Grabowska, D. B. Kaplan and S. Reddy, Phys. Rev. D **91**, no. 8, 085035 (2015) doi:10.1103/PhysRevD.91.085035 [arXiv:1409.3602 [hep-ph]].
- [34] M. Kaminski, C. F. Uhlemann, M. Bleicher and J. Schaffner-Bielich, Phys. Lett. B **760**, 170 (2016) doi:10.1016/j.physletb.2016.06.054 [arXiv:1410.3833 [nucl-th]].
- [35] G. Sigl and N. Leite, JCAP **1601**, no. 01, 025 (2016) doi:10.1088/1475-7516/2016/01/025 [arXiv:1507.04983 [astro-ph.HE]].
- [36] N. Yamamoto, Phys. Rev. D **93**, no. 6, 065017 (2016) doi:10.1103/PhysRevD.93.065017 [arXiv:1511.00933 [astro-ph.HE]].
- [37] Y. Masada, K. Kotake, T. Takiwaki and N. Yamamoto, Phys. Rev. D **98**, no. 8, 083018 (2018) doi:10.1103/PhysRevD.98.083018 [arXiv:1805.10419 [astro-ph.HE]].

- [38] Q. Li *et al.*, Nature Phys. **12**, 550 (2016) doi:10.1038/nphys3648 [arXiv:1412.6543 [cond-mat.str-el]].
- [39] B. Q. Lv *et al.*, Phys. Rev. X **5**, no. 3, 031013 (2015) doi:10.1103/PhysRevX.5.031013 [arXiv:1502.04684 [cond-mat.mtrl-sci]].
- [40] S. Y. Xu *et al.*, Science **349**, 613 (2015). doi:10.1126/science.aaa9297
- [41] K. Nishiyama, S. Karasawa and T. Tatsumi, Phys. Rev. D **92**, 036008 (2015) doi:10.1103/PhysRevD.92.036008 [arXiv:1505.01928 [nucl-th]].
- [42] H. Abuki, EPJ Web Conf. **129**, 00036 (2016) doi:10.1051/epjconf/201612900036 [arXiv:1609.04605 [hep-ph]].
- [43] H. Abuki, JPS Conf. Proc. **20**, 011017 (2018). doi:10.7566/JPSCP.20.011017
- [44] M. Kawaguchi, Y. L. Ma and S. Matsuzaki, Phys. Rev. C **98**, no. 3, 035803 (2018) doi:10.1103/PhysRevC.98.035803 [arXiv:1804.09015 [nucl-th]].
- [45] J. Wess and B. Zumino, Phys. Lett. **37B**, 95 (1971). doi:10.1016/0370-2693(71)90582-X
- [46] E. Witten, Nucl. Phys. B **223**, 422 (1983). doi:10.1016/0550-3213(83)90063-9
- [47] K. Fukushima and K. Mameda, Phys. Rev. D **86**, 071501 (2012) doi:10.1103/PhysRevD.86.071501 [arXiv:1206.3128 [hep-ph]].
- [48] G. Cao and X. G. Huang, Phys. Lett. B **757**, 1 (2016) doi:10.1016/j.physletb.2016.03.066 [arXiv:1509.06222 [hep-ph]].
- [49] T. H. R. Skyrme, “A Unified Field Theory of Mesons and Baryons,” Nucl. Phys. **31**, 556 (1962). doi:10.1016/0029-5582(62)90775-7
- [50] I. R. Klebanov, Nucl. Phys. B **262**, 133 (1985). doi:10.1016/0550-3213(85)90068-9
- [51] E. Witten, Nucl. Phys. B **223**, 433 (1983). doi:10.1016/0550-3213(83)90064-0
- [52] C. Naya and P. Sutcliffe, Phys. Rev. Lett. **121**, no. 23, 232002 (2018) doi:10.1103/PhysRevLett.121.232002 [arXiv:1811.02064 [hep-th]].
- [53] H. J. Lee, B. Y. Park, D. P. Min, M. Rho and V. Vento, “A Unified approach to high density: Pion fluctuations in skyrmion matter,” Nucl. Phys. A **723**, 427 (2003) doi:10.1016/S0375-9474(03)01452-0 [hep-ph/0302019].
- [54] H. J. Lee, B. Y. Park, M. Rho and V. Vento, Nucl. Phys. A **741**, 161 (2004) doi:10.1016/j.nuclphysa.2004.06.010 [hep-ph/0307111].
- [55] Y. L. Ma, M. Harada, H. K. Lee, Y. Oh, B. Y. Park and M. Rho, Phys. Rev. D **88**, no. 1, 014016 (2013) Erratum: [Phys. Rev. D **88**, no. 7, 079904 (2013)] doi:10.1103/PhysRevD.88.014016, 10.1103/PhysRevD.88.079904 [arXiv:1304.5638 [hep-ph]].
- [56] Y. L. Ma, M. Harada, H. K. Lee, Y. Oh, B. Y. Park and M. Rho, Phys. Rev. D **90**, no. 3, 034015 (2014) doi:10.1103/PhysRevD.90.034015 [arXiv:1308.6476 [hep-ph]].
- [57] B. Y. Park and V. Vento, Skyrmion approach to finite density and temperature in *The Multifaceted Skyrmion (2nd edition)* (World Scientific, Singapore, 2017), ed. M. Rho and I. Zahed.
- [58] Y. L. Ma and M. Harada, arXiv:1604.04850 [hep-ph].
- [59] Y. L. Ma and M. Rho, Sci. China Phys. Mech. Astron. **60**, no. 3, 032001 (2017) doi:10.1007/s11433-016-0497-2 [arXiv:1612.06600 [nucl-th]].
- [60] M. Harada, H. K. Lee, Y. L. Ma and M. Rho, “Inhomogeneous quark condensate in compressed Skyrmion matter,” Phys. Rev. D **91**, no. 9, 096011 (2015) doi:10.1103/PhysRevD.91.096011 [arXiv:1502.02508 [hep-ph]].
- [61] M. Kawaguchi, Y. L. Ma and S. Matsuzaki, arXiv:1810.12880 [nucl-th].
- [62] W. G. Paeng, T. T. S. Kuo, H. K. Lee, Y. L. Ma and M. Rho, Phys. Rev. D **96**, no. 1, 014031 (2017) doi:10.1103/PhysRevD.96.014031 [arXiv:1704.02775 [nucl-th]].
- [63] Y. L. Ma, H. K. Lee, W. G. Paeng and M. Rho, arXiv:1804.00305 [nucl-th].
- [64] Y. L. Ma and M. Rho, Phys. Rev. D **99**, no. 1, 014034 (2019) doi:10.1103/PhysRevD.99.014034 [arXiv:1810.06062 [nucl-th]].
- [65] D. T. Son and A. R. Zhitnitsky, Phys. Rev. D **70**, 074018 (2004) doi:10.1103/PhysRevD.70.074018 [hep-ph/0405216].
- [66] D. T. Son and M. A. Stephanov, Phys. Rev. D **77**, 014021 (2008) doi:10.1103/PhysRevD.77.014021 [arXiv:0710.1084 [hep-ph]].
- [67] B. R. He, Phys. Rev. D **92**, no. 11, 111503 (2015) doi:10.1103/PhysRevD.92.111503 [arXiv:1510.04683 [hep-ph]].